Superpixel and Entropy-Based Multi-atlas Fusion Framework for the Segmentation of X-ray Images

Dac Cong Tai Nguyen[2,3], Said Benameur[2,3](✉), Max Mignotte[2], and Frédéric Lavoie[1,3]

[1] Orthopedic Surgery Department, Centre Hospitalier de l'Université de Montréal (CHUM), Montréal, Québec, Canada
[2] Département d'Informatique et de Recherche Opérationnelle (DIRO), Université de Montréal, Québec, Canada
[3] Eiffel Medtech Inc., Montréal, Québec, Canada
dac.cong.tai.nguyen@umontreal.ca, benameus@iro.umontreal.ca

Abstract. X-ray images segmentation can be useful to aid in accurate diagnosis or faithful 3D bone reconstruction but remains a challenging and complex task, particularly when dealing with large and complex anatomical structures such as the human pelvic bone. In this paper, we propose a multi-atlas fusion framework to automatically segment the human pelvic structure from 45 or 135-degree oblique X-ray radiographic images. Unlike most atlas-based approach, this method combines a data set of a priori segmented X-ray images of the human pelvis (or multi-atlas) to generate an adaptive superpixel map in order to take efficiently into account both the imaging pose variability along with the inter-patient (bone) shape non-linear variability. In addition, we propose a new label propagation or fusion step based on the variation of information criterion for integrating the multi-atlas information into the final consensus segmentation. We thoroughly evaluated the method on 30 manually segmented 45 or 135 degree oblique X-ray radiographic images data set by performing a leave-one-out study. Compared to the manual gold standard segmentations, the accuracy of our automatic segmentation approach is 85% which remains in the error range of manual segmentations due to the inter intra/observer variability.

Keywords: Consensus segmentation · X-ray images · Multi-atlas segmentation · Variation of information based fusion step · Superpixel map

1 Introduction

In clinical practice, X-Ray radiographic images are used to assist in disease diagnosis, pre-operative planning and treatment analysis. Extraction of the contours and/or regions of the bone structures (pelvis, talus, patella, etc.) from 45-degree and 135-degree oblique X-Ray radiographic images may eventually play

V. Murino and E. Puppo (Eds.): ICIAP 2015, Part II, LNCS 9280, pp. 151–161, 2015.
DOI: 10.1007/978-3-319-23234-8_15

an important role in the diagnosis and treatment of diseases such as osteoarthritis (e.g. joint-replacement planning) or osteoporosis (e.g. fracture detection and bone density measurements).

X-Ray segmentation of bone structures in the pelvic region is both intrinsically and extrinsically difficult. This is caused partly by the intrinsic difficulties of the system. First because of the X-Ray imaging systems: Noise in X-Ray images has a number of origins, but the most fundamental is from the X-Ray source itself. This type of noise is called quantum noise, in reference to the discrete nature of the X-Ray photons producing it. Also, bone regions in X-Ray images often overlap with soft tissues and other bones. Extrinsic difficulties are usually due to the patients: neighboring tissues inside human body may have similar X-Ray absorption rates. As a result, the boundaries of the organs may be ambiguous and there is sometimes no clear edge between two neighboring bone structures. In addition we must also consider the bone structures density variability, the inter-patient (bone structure) shape variability and the imaging pose variability. These difficulties are particularly true when dealing with large and complex anatomical structures such as the human pelvic bone which explains why the segmentation process of such anatomical structures is currently performed manually or semi-automatically and often requires human expert interaction.

To simplify and guide an automatic segmentation task, *a priori* anatomical information is essential and may be provided in different ways. For instance, with the knowledge of the luminance distributions within each different tissue or regions to be segmented [1] or in the form of deformable statistical models represented by a family of parametrized curves [2,3] or by one or several prototype templates together with their parametric spaces of deformations [4].

A recent, simple and non-parametric alternative to bring spatial prior knowledge to the segmentation process consists in defining and using a multi-atlas, *i.e.*, a set of training segmented images (possibly with the set of their associated X-ray images) [5–7]. With this latest strategy, the automatic segmentation task turns into a two step procedures; namely a first registration step where each atlas segmented (possibly with its associated X-ray image) is registered to the target image independently and the calculated transformation is then applied to the segmentation of the atlas image to obtain a segmented version of the target image and a second *fusion* or *label propagation* step where the preceding candidate segmentations, resulting from the first step, are finally fused to produce a final consensus segmentation.

More precisely, in the multi-atlas segmentation strategy, the first registration stage is usually carried out in two steps: a global rigid registration that obtains an initial rough alignment followed by a local non-rigid (and non-linear) registration to take into account the target specific deformation (mainly due to inter-patient bone structure and imaging pose variability). This latter non-linear registration is typically performed by applying a non-linear parametric transform model on the control points of a free-form deformation grid with B-spline-curves, demons, optical flows, etc. [8]. In these commonly used registration strategies, it is important to note that the parametric deformation model is generally computationally expensive, could fail in the case of complex deformations and is not learned from the multi-atlas data set. In this work, the multi-atlas allows us to generate an adaptive superpixel map which is then exploited to efficiently take into account the non linear target-specific deformations and to comprise all the non-linear variability of the multi-atlas population.

Concerning the second *fusion* or *label propagation* step, the commonly used combination strategies, proposed in the literature, include majority voting [9], (possibly locally) weighted voting [5] or Expectation-Maximization algorithm based vote procedure[10]. In this study, we propose to use a *label propagation* strategy based on the minimization of the variation of information criterion [11] between the candidate segmentations to be fused. This fusion procedure has already turned out to be very relevant for combining multiple low cost and inaccurate segmentations given by several simple algorithms of a textured natural image to achieve a final improved segmentation [11].

2 Proposed Model

2.1 Data Set and Multi-atlas Creation

Anonymised 45 and 135 degree oblique X-ray radiographic images of the full pelvic bone from 31 patients without pelvic deformity were obtained after approval by the local ethics board. Images of the pelvis were manually segmented into 14 different regions of interest (ROIs) by experts well trained in pelvic anatomy and medical image segmentation. These segmentations included the entire pelvis with all three adjoining bones, namely the left and right proximal femurs as well as the sacrum including the coccyx (tail bone). Each hemipelvis consists of the ischium, the ilium and the pubis (see Fig. 1).

2.2 Image Pre-processing

All the acquired X-Ray images to be segmented are firstly pre-processed with a histogram equalization technique and a DCT-based denoising step [12,13] to enhance the contour of the different bones of the human pelvis region. These contour cues will be then exploited in the contour-based registration step explained in the following section.

2.3 Proposed Multi-atlas Fusion Procedure

Linear Registration and Multi-atlas Selection Step. As said in Introduction, the most informative and reliable visual cues in a X-Ray image of the pelvic region remains the boundary contours between the different pelvic bone structures and particularly the external bone contour of the pelvis. Considering this, each atlas segmented image is linearly registered to the target image independently

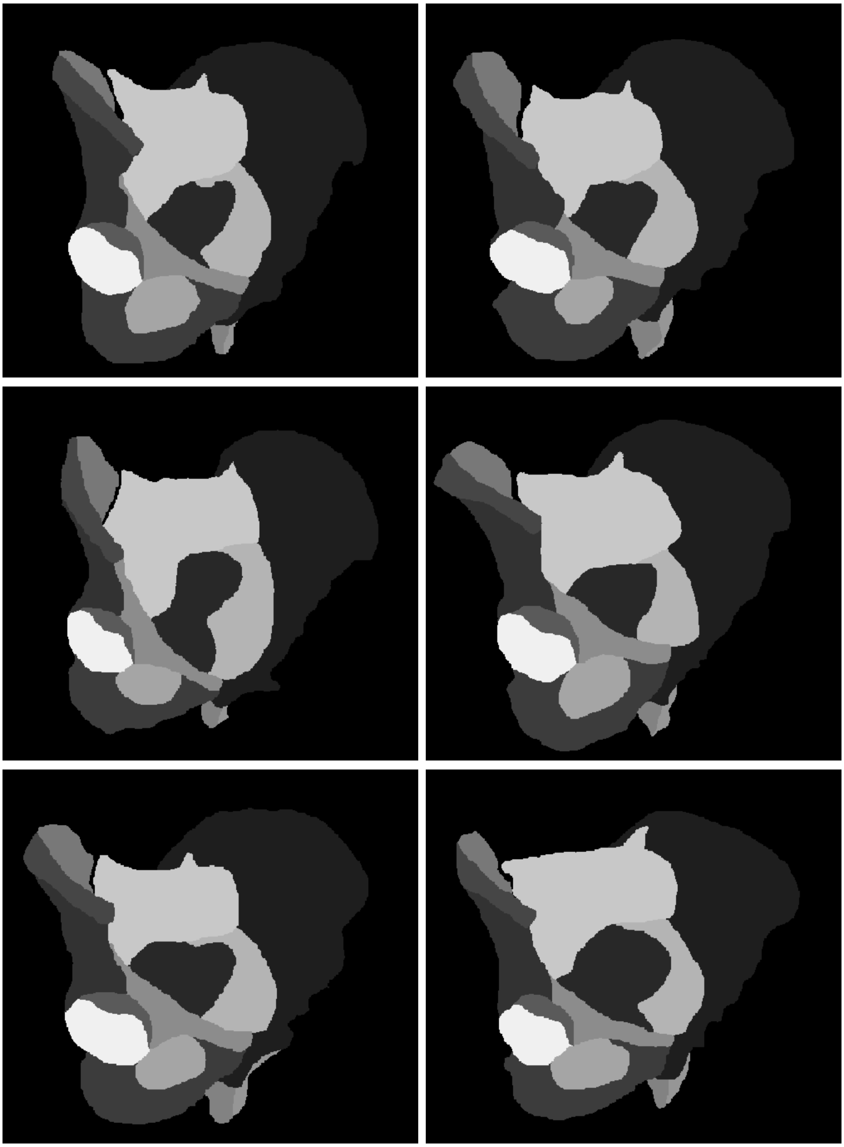

Fig. 1. 6 examples of 45-degree oblique manual segmentations of the human pelvic bone used in our multi-atlas.

using a contour-based registration technique. More precisely, a global linear registration (affine or rigid transformations) is performed to obtain an initial alignment that maximizes a measure of similarity between the external contour of the pelvis region in the segmented image of the atlas and an edge potential field (edge map) estimated on the X-Ray image by a simple Canny edge detector (allowing to

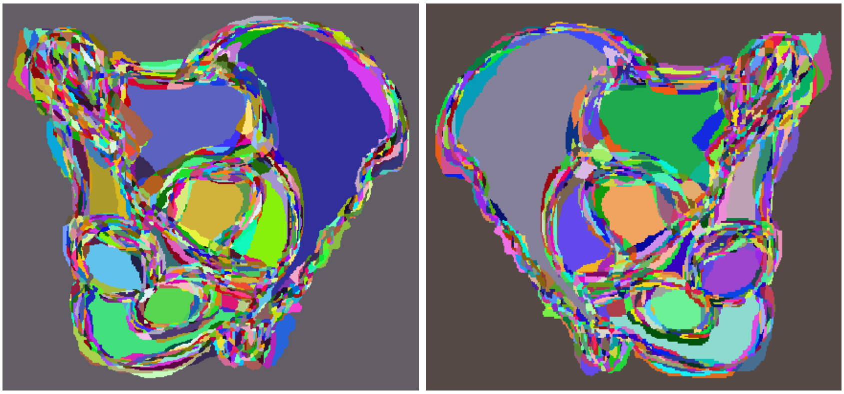

Fig. 2. Superpixel maps obtained for a given X-ray 45 and 135 degree image to be segmented.

obtain a binary edge image) [14] followed by a Gaussian blur (filter) with standard deviation σ controlling the degree of smoothness of this edge potential map [15]. The global rigid registration that maximizes the summation of this potential map over all the pixels on the boundary of the external contour of the pelvis (given by the manual segmentation) thus allows to obtain a rough alignment of each atlas image to the target image.

In addition, our contour-based similarity registration metric allows us to rank the different manual segmentations of our multi-atlas by decreasing order of similarity and consequently to select the first half of the segmented images of the multi-atlas for generating the superpixel map which will be explained in the following section.

Superpixel Map Creation. The first half of the segmented images of the multi-atlas allows us to generate a superpixel map where each defined superpixel remains a coherent unit which, in fact, contains a set of connected pixels belonging to the same label region for each segmented image of our subset (i.e., pre-selected as previously mentioned) of manual segmented images of the multi-atlas. This superpixel map is simply obtained by the intersection of all the regions (or segments) existing in the multi-atlas (see Fig. 2).

The use of superpixel was originally developed by Ren and Malik in [16] as a pre-processing step for the segmentation of natural images [16] in order to reduce the number of entities to be labeled when the segmentation is formulated as a difficult optimization problem (in the space of all possible segmentations). Let us also note that the use of superpixels in an energy-based fusion procedure has also been initially proposed in [17] with a different goal, namely the one of blending a spatial segmentation (region map) and a quickly estimated and to-be-refined application field (e.g., motion estimation/segmentation field, occlusion map, etc.) and in [18] for restoration application.

In our application, the superpixel map is thus adaptive for each X-Ray target image to be segmented and will allow us to carry out an adaptive local non-rigid registration to take into account the non linear target-specific deformations. This will be explained in the following section.

Non-linear Registration from the Superpixel Map. Each X-Ray target image allows us to generate a specific superpixel map which locally comprises all the non-linear variability (*i.e.*, inter-patient bone structure and imaging pose variability) of a selected subset of the multi-atlas population (see the selection step in section 2.3). To this end, let us recall that the subset of selected segmented images, used to generate the superpixel map, have been linearly registered to the target image. By this fact, the superpixel map is already linearly registered to the target image. An iterative pruning algorithm is then defined to find the set of connected superpixels which maximizes the contour-based similarity measure between the edge map of the target X-Ray image and the outer contour of this superpixel map[1].

More precisely, each superpixel, in a lexicographic order, which is connected with the background label (*i.e.*, which is contiguous with the external region of the pelvic bone), is considered as belonging to the pelvic region if the outer contour-based similarity metric increases and until convergence or a maximum number of iterations is reached. At convergence, this pruning algorithm allows us to find an accurate closed external contour of the pelvic bone which is then used in the following step.

Final Selection and Variation of Information Based Fusion Step. A final linear registration between the previously closed external contour allows us to select the first quarter of the manual segmentations of our multi-atlas data set, in term of a region-based similarity metric, and to fuse these segmentations in the variation of information (VoI) sense [11]. This similarity metric is the F-measure (the harmonic mean of precision and recall) between the internal region defined by the previously estimated closed external contour and the internal region of the pelvis (given by the manual segmentation).

In this *label propagation* step, the VoI-based fusion procedure allows to infer the internal region labels of the pelvis from the filtered (or selected) atlases to the final segmentation image.

[1] Experiments have shown that slightly better results are given if the superpixel map is scaled by a factor slightly greater than one in order to ensure that the pelvis contour of the X-Ray target image is fully contained in the superpixel map. To this end, after trial and error, a scale factor of 1.02 allows us to give the best segmentation results.

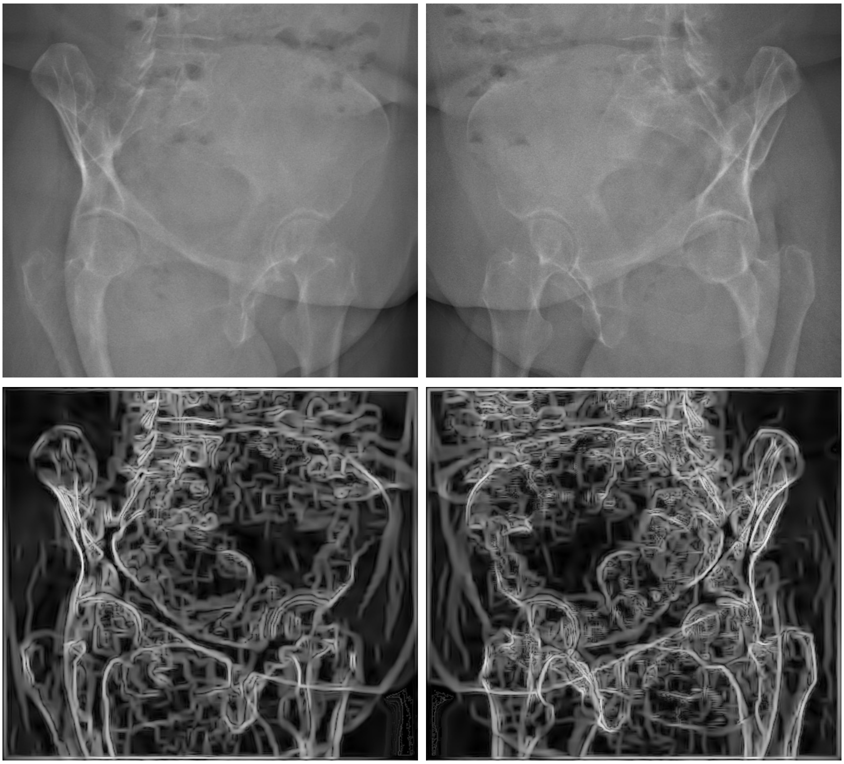

Fig. 3. Original oblique X-Ray radiographic images of pelvis before and after the pre-processing step (see Section 2.2: the pre-processing step).

3 Experimental Results

In all the experiments, we have tested our multi-atlas segmentation approach on 31 images (45 or 135-degree oblique) X-ray radiographic images of the pelvis acquired using a X-ray imaging system (see Fig. 3).

In order to validate our procedure, we have performed a leave-one-out procedure, *i.e.,* we removed each existing manual segmentation from the multi-atlas data set while other manual segmentations remained. Each X-Ray image associated to the previously removed segmentation map was then segmented by our strategy and compared, in terms of classification error rate, with its manual segmentation. Compared to the manual gold standard segmentations, the accuracy of our automatic segmentation approach was 85%. Examples of segmentations are given in Figures 4 and 5. Figure 6 shows two segmentation results from our automatic segmentation approach compared to a manual gold standard segmentation. In this example, the accuracy of our automatic segmentation approach is respectively 89% for Figure 6(g), 85% for Figure 6(h), 81% for Figure 6(i).

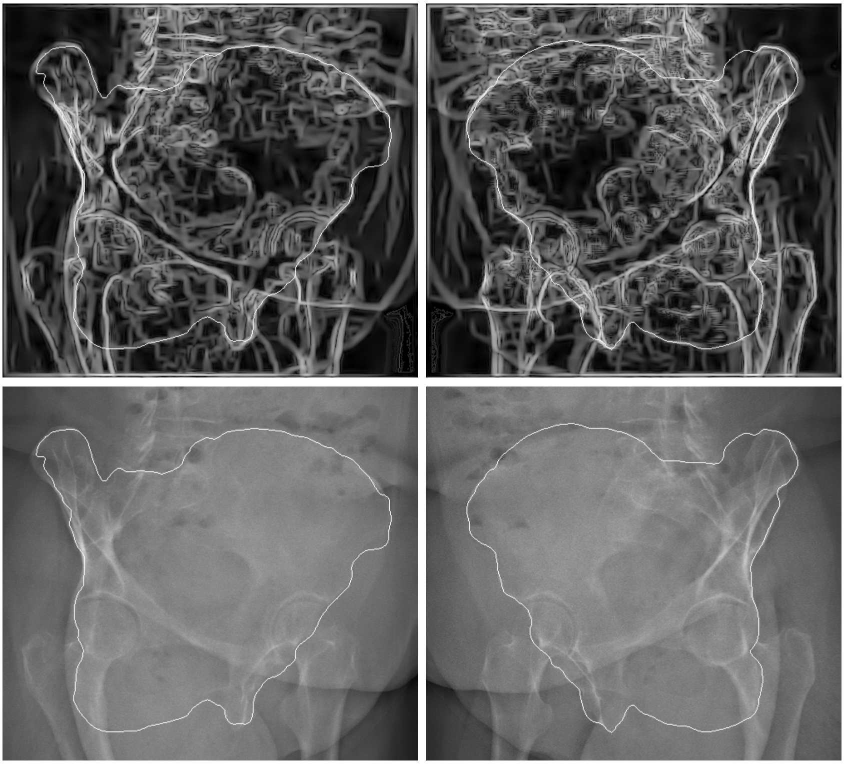

Fig. 4. Example of external pelvis contours on the corresponding 45 and 135 -degree oblique X-ray radiographic (original and gradient) images.

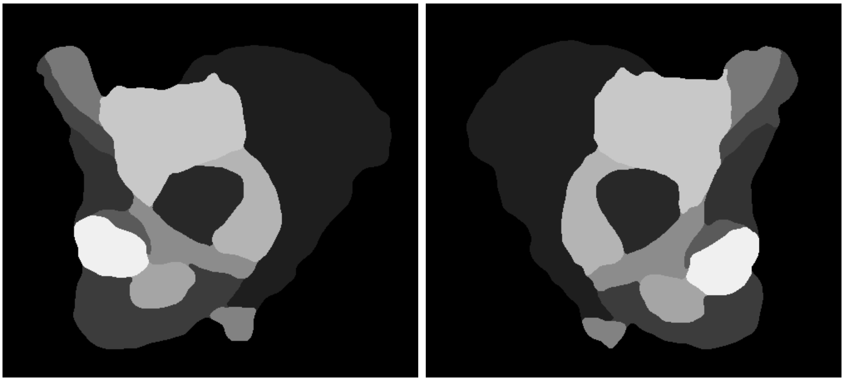

Fig. 5. Resulting fusion image estimated after the VoI-based *label propagation* step, with the estimated internal region labels of the pelvis.

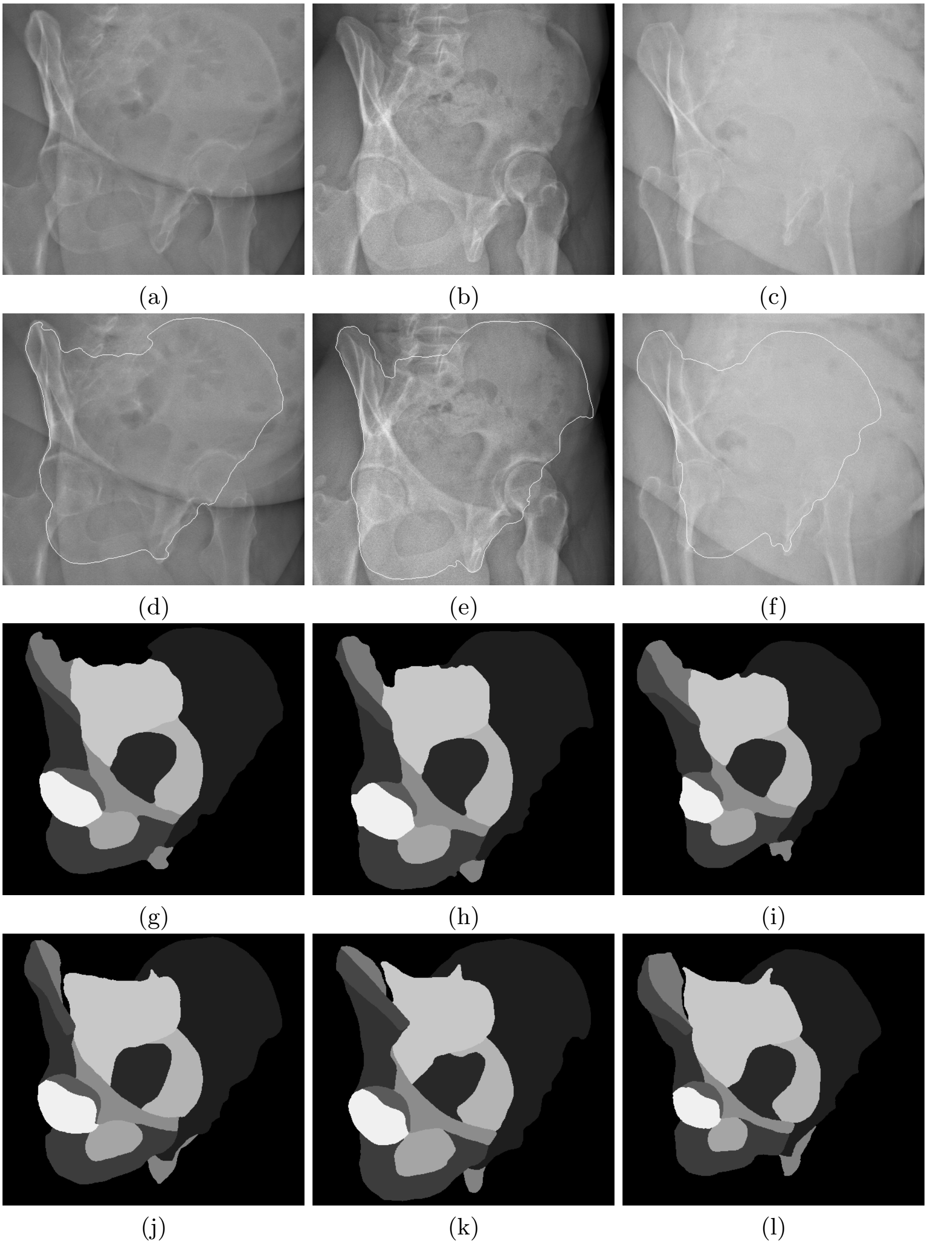

Fig. 6. Comparison of two segmentation results from our automatic segmentation approach and a manual gold standard. (a),(b) and (c) original oblique X-Ray radiographic images of pelvis; (d),(e) and (f) external pelvis contours on the corresponding 45 -degree oblique X-ray radiographic images; (g),(h) and (i) resulting fusion image estimated after the VoI-based *label propagation* step, with the estimated internal region labels of the pelvis; (j),(k) and (l) a manual segmentations of the corresponding 45 -degree oblique X-ray radiographic images

4 Conclusion

In this paper, a new multi-atlas based segmentation method is presented. Unlike most atlas-based approach, the proposed method includes the following contributions. First, the multi-atlas data set allows us to generate an adaptive superpixel map which comprises all the non-linear variability of the multi-atlas population and allows us to take into account the non linear target-specific deformations of our multi-atlas based segmentation approach. Second, the similarity measure used in our registration step is used in an atlas selection strategy both for the registration step and for the label propagation fusion step, which is herein performed in the variation of information sense. Third our approach allows us to consider only the most informative and reliable visual cues in a X-Ray image of the pelvic region, *i.e.,* the external bone contour of the pelvis and the *fusion* step then allows to infer the internal region labels of the pelvis from the filtered (or selected) atlases to the final segmentation image. The average classification rate, obtained with a leave-one-out method, is within the range of observer variability when compared to a semi-automatic segmentation technique that is performed by an expert.

References

1. Mignotte, M., Collet, C., Pérez, P., Bouthemy, P.: Sonar image segmentation using an unsupervised hierarchical MRF model. IEEE Trans. on Image Processing **9**(7), 1216–1231 (2000)
2. Mignotte, M., Meunier, J., Tardif, J.-C.: Endocardial boundary estimation and tracking in echocardiographic images using deformable templates and markov random fields. Pattern Analysis and Applications **4**(4), 256–271 (2001)
3. Mignotte, M., Meunier, J.: A multiscale optimization approach for the dynamic contour-based boundary detection issue. Computerized Medical Imaging and Graphics **25**(3), 265–275 (2001)
4. Destrempes, F., Mignotte, M.: Localization of shapes using statistical models and stochastic optimization. IEEE Trans. on Pattern Analysis and Machine Intelligence **29**(9), 1603–1615 (2007)
5. Artaechevarria, X., Muñoz-Barrutia, A., Ortiz-de-Solorzano, C.: Combination strategies in multi-atlas image segmentation: Application to brain MR data. IEEE Trans. Med. Imaging **28**(8), 1266–1277 (2009)
6. Aljabar, P., Heckemann, R.A., Hammers, A., Hajnal, J.V., Rueckert, D.: Multi-atlas based segmentation of brain images: Atlas selection and its effect on accuracy. NeuroImage, 726–738 (2009)
7. Dowling, J.A., Fripp, J., Chandra, S., Pluim, J.P.W., Lambert, J., Parker, J., Denham, J., Greer, P.B., Salvado, O.: Fast automatic multi-atlas segmentation of the prostate from 3D MR images. In: Madabhushi, A., Dowling, J., Huisman, H., Barratt, D. (eds.) Prostate Cancer Imaging 2011. LNCS, vol. 6963, pp. 10–21. Springer, Heidelberg (2011)
8. Morin, J.-P., Desrosiers, C., Duong, L.: A random walk approach for multiatlas-based segmentation. In: ICPR 2012, pp. 3636–3639 (2012)

9. Rohlfing, T., Brandt, R., Menzel, R., Maurer, C.R.: Evaluation of atlas selection strategies for atlas-based image segmentation with application to confocal microscopy images of bee brains. Neuroimage **21**(4), 1428–1442 (2004)
10. Rohlfing, T., Russakoff, D.B., Maurer, C.R.: Performance-based classifier combination in atlas-based image segmentation using expectation-maximization parameter estimation. IEEE Trans. Med. Imaging **23**(8), 983–994 (2004)
11. Mignotte, M.: A label field fusion model with a variation of information estimator for image segmentation. Information Fusion **20**, 7–20 (2014)
12. Mignotte, M., Meunier, J., Soucy, J.-P.: DCT-based complexity regularization for EM tomographic reconstruction. IEEE Trans. on Biomedical Engineering **55**(2), 801–805 (2008)
13. Yu, G., Sapiro, G.: DCT image denoising: a simple and effective image denoising algorithm. Image Processing On Line **1** (2011)
14. Canny, J.: A computational approach to edge detection. IEEE Transactions on Pattern Analysis and Machine Intelligence **8**(6), 679–698 (1986)
15. Benameur, S., Mignotte, M., Parent, S., Labelle, H., Skalli, W., De Guise, J.: 3d/2d registration and segmentation of scoliotic vertebrae using statistical models. Computerized Medical Imaging and Graphics **27**(5), 321–327 (2003)
16. Ren, X., Malik, J.: Learning a classification model for segmentation. In: 9th IEEE International Conference on Computer Vision, vol. 1, pp. 10–17 (October 2003)
17. Jodoin, P.-M., Mignotte, M., Rosenberger, C.: Segmentation framework based on label field fusion. IEEE Trans. on Image Processing **16**(10), 2535–2550 (2007)
18. Mignotte, M.: A segmentation-based regularization term for image deconvolution. IEEE Trans. on Image Processing **15**(7), 1973–1984 (2006)